

# 72 DA White Dwarfs Identified in LAMOST Pilot Survey

J. K. Zhao<sup>1</sup>, A. L. Luo<sup>1</sup>, T.D. Oswalt<sup>2</sup>, G. Zhao<sup>1</sup>

## ABSTRACT

We present a spectroscopically identified catalogue of 72 DA white dwarfs from the LAMOST pilot survey. 35 are found to be new identifications after cross-correlation with the Eisenstein et al. and Villanova catalogues. The effective temperature and gravity of these white dwarfs are estimated by Balmer lines fitting. Most of them are hot white dwarfs. The cooling times and masses of these white dwarfs are estimated by interpolation in theoretical evolution tracks. The peak of mass distribution is found to be  $\sim 0.6 M_{\odot}$  which is consistent with prior work in the literature. The distances of these white dwarfs are estimated using the method of Synthetic Spectral Distances. All of these WDs are found to be in the Galactic disk from our analysis of space motions. Our sample supports the expectation white dwarfs with high mass are concentrated near the plane of Galactic disk.

*Subject headings:* white dwarfs: Stars

## 1. Introduction

White dwarfs (WDs) are the final stage for the the evolution of majority of low and medium mass stars with initial masses  $< 8M_{\odot}$ . Since there are no fusions reaction, the evolution of WDs is primarily determined by a well understood cooling process (Fontaine et al. 2001; Salaris et al. 2000). Thus, they can be used for cosmochronology, an independent age-dating method. Also, the luminosity function of WDs provides firm constraints on the local star formation rate and history of the Galactic disk (Krziesinski et al. 2009).

McCook & Sion (1999) present a catalog of 2249 WDs which have been identified spectroscopically. In addition, the Sloan Digital Sky Survey (SDSS; York et al. 2000) has greatly

---

<sup>1</sup>Key Laboratory of Optical Astronomy, National Astronomical Observatories, Chinese Academy of Sciences, Beijing, 100012, China; zjk@bao.ac.cn, gzhao@bao.ac.cn, lal@bao.ac.cn

<sup>2</sup>Physics and Space Science Department, Florida Institute of Technology, Melbourne, USA, 32901, toswalt@fit.edu

expanded the number of spectroscopically confirmed WD stars (Harris et al. 2003; Kleinman et al. 2004; Eisenstein et al. 2006; Kleinman et al. 2013). The latter presented a catalog of 20,407 spectroscopically confirmed white dwarfs from the SDSS Data Release 4 (DR4), roughly doubling the number of spectroscopically confirmed white dwarfs.

Large sky Area Multi-Object Fiber Spectroscopic Telescope (LAMOST, so called the Guoshoujing Telescope) is a National Major Scientific Project undertaken by the Chinese Academy of Science (Wang et al. 1996; Cui et al. 2012). LAMOST has recently completed the pilot survey from October 2011 to May 2012, which obtained several hundred thousand spectra (Luo et al. 2012). From September of 2012, LAMOST has undertaken the general survey and will observe about 1 million stars per year. LAMOST has the capability to observe large, deep and dense regions in the Milky Way Galaxy, which will enable a number of research topics to explore the evolution and the structure of the Milky Way. Therefore, it will definitely yield a large sample of WDs.

WDs whose primary spectral classification is DA have hydrogen-dominated atmospheres. They make up the majority (approximately 75%) of all observed WDs (Fontaine & Wesemael 2001). Such WDs are easy to identify using optical spectra. Here we present a catalog of DA WDs from the LAMOST pilot survey (Luo et al. 2012). **We do not expect the completeness of this sample.** In section 2 we describe the spectra obtained. Section 3 discusses how the  $T_{\text{eff}}$ ,  $\log g$ , mass and distance of the WDs were estimated. The kinematics of these WDs are illustrated in section 4. A summary of our pilot study results is given in section 5.

## 2. LAMOST Pilot Data and Observations

The LAMOST spectra have a resolving power of  $R \sim 2000$  spanning  $3700\text{\AA} \sim 9000\text{\AA}$ . Two arms of each spectrograph cover this wavelength range with overlap of  $200\text{\AA}$ . The blue spectral coverage is  $3700\text{\AA} \sim 5900\text{\AA}$  while that in the red is  $5700\text{\AA} \sim 9000\text{\AA}$ . The raw data were reduced with LAMOST 2D and 1D pipelines (Luo et al. 2004). These pipelines include bias subtraction, cosmic-ray removal, spectral trace and extraction, flat-fielding, wavelength calibration, sky subtraction, and combination. The throughput in red is higher than the blue band.

The pilot survey obtained spectra of stars in the Milky Way, which included fainter objects on dark nights (Yang et al. 2012; Carlin et al. 2012), brighter objects on bright nights (Zhang et al. 2012), objects in the disk of the Galaxy with low latitude (Chen et al. 2012) and objects in the region of the Galactic Anti-Center. It also targets extragalactic

objects located in two regions, i.e., the South Galactic Cap and the North Galactic Cap.

We found twenty WD spectra in both SDSS and LAMOST pilot survey catalogs. Fig. 1 shows a portion of a typical spectrum. The top panel compares the SDSS DR7 and LAMOST spectra for the object J100316.35-002336.95. The solid line is the SDSS spectrum. The dotted line is the LAMOST spectrum. The bottom panel shows the residual between two spectra. The mean difference between two spectra is less than 10 %.

The initial WD candidates we selected are from two sources. One is the LAMOST pipeline (Luo et al. 2012) which yielded about 2000 candidates using the "PCAZ" method. For stars with SDSS photometry, we used the formulas 1-4 of Elsenstein et al. (2006) to identify candidates. Next, each of these spectra was inspected by eye. Stars with signal-to-noise ratio (S/N) smaller than 10 were excluded. Finally, if the Balmer line profiles of the star were a little too narrow ( $\log g < 7.0$ ), the spectrum was rejected even if selected by the pipeline. After these filters, 72 DA WDs were left. Table 1 presents the physical data for these WDs. Column 1 is an ID number. Columns 2-5 list the name, RA and DEC. The estimated  $T_{\text{eff}}$ ,  $\log g$ , mass and the cooling time are given in columns 5-8. Columns 9-13 list the apparent magnitudes of each WDs. Column 14 indicates the source of the magnitudes. The last two columns are estimates of the color excess (B-V) and distance. The E(B-V) is estimated from Schlegel et al. (1998).

### 3. Parameter Determination

#### 3.1. $T_{\text{eff}}$ and $\log g$

For our DA WD candidates, the  $T_{\text{eff}}$  and  $\log g$  were derived via simultaneous fitting of the H $\beta$  to H8 Balmer line profiles using the procedure outlined by Bergeron et al. (1992). The line profiles in both observed spectra and model spectra were first normalized using two points at the continuum level on either side of each absorption line. Thus, the fit should not be affected by the flux calibration. Model atmospheres used for this fitting were derived from model grids provided by Koester (2010). Details of the input physics and methods can be found in that reference. Fitting of the line profiles was carried out using the IDL package MPFIT (Markwardt 2008), which is based on  $\chi^2$  minimization using Levenberg-Marquardt method. This package can be downloaded from the project website<sup>1</sup>. Errors in the  $T_{\text{eff}}$  and  $\log g$  were calculated by stepping the parameter in question away from their optimum values and redetermining minimum  $\chi^2$  until the difference between this and the true minimum  $\chi^2$

---

<sup>1</sup><http://purl.com/net/mpfit>

corresponded to  $1\sigma$  for a given number of free model parameters.

Figs. 2-3 show examples of  $T_{\text{eff}}$  and  $\log g$  determinations for J150156.26+302300.13. Fig.2 is the contour plot of the  $\chi^2$  residual and the rough  $T_{\text{eff}}$  and  $\log g$  implied by these error eclipses. Fig. 3 shows the actual fits of the observed Balmer lines for J150156.26+302300.13. The black solid lines are the observed profiles of Balmer lines from  $H\beta$  to H8. The red dashed lines are the model spectra. The derived  $T_{\text{eff}}$ ,  $\log g$  and uncertainties for all the WDs are shown in columns 5-6 of Table 1. Estimated  $T_{\text{eff}}$  and  $\log g$  values for 14 DAs were also available in the literature, allowing the comparisons shown in Fig. 4. The solid line represents the unit slope relation. Plus (+) symbols represent the WDs with high S/N spectra while squares represent WDs with low S/N spectra. The three spectra of lowest S/N are outliers in the  $\log g$  comparison plot-suggesting the importance of S/N in determining this parameter. For most of other WDs, the mean differences between our and the literature  $T_{\text{eff}}$  values are less than 1000 K and the  $\log g$  difference is less than 0.2 dex. Within this scatter, our results are consistent with those in the literatures. One of our candidates, J104311.45+490224.35 has also been identified as DA WD by McCook & Sion (1999). However, we were unable to determine its  $T_{\text{eff}}$  and  $\log g$  because  $H\beta$  was not included in the spectrum we obtained.

### 3.2. Mass and Cooling Time

From the  $T_{\text{eff}}$  and  $\log g$  of each WD, its mass ( $M_{\text{WD}}$ ) and cooling time ( $t_{\text{cool}}$ ) were estimated from Bergeron’s cooling sequences<sup>2</sup>. For the model atmospheres above  $T_{\text{eff}} = 30,000$  K we used the carbon-core cooling models of Wood (1995), with thick hydrogen layers of  $q_{\text{H}} = M_{\text{H}}/M_{\star} = 10^{-4}$ . For  $T_{\text{eff}}$  below 30,000 K we used cooling models similar to those described in Fontaine, Brassard & Bergeron (2001) but with carbon-oxygen cores and  $q_{\text{H}} = 10^{-4}$  (see Bergeron, Leggett & Ruiz 2001).

Fig. 5 is the mass distribution of our sample resulting from the above procedure. Masses are found to range from  $0.4 M_{\odot}$  to  $1.2 M_{\odot}$ . The curve is a Gaussian fit with a peak at about  $0.61 M_{\odot}$ , which is consistent with the mean mass  $0.613 M_{\odot}$  from Tremblay et al. (2011) derived from SDSS DA WDs sample.

---

<sup>2</sup>The cooling sequences can be downloaded from the website: <http://www.astro.umontreal.ca/~bergeron/CoolingModels/>.

### 3.3. Distance

The determination of distances for WDs is very difficult because of their low luminosity. Currently only about 300 WDs have trigonometric parallaxes. In the absence of parallaxes, color-magnitude relations and empirical photometric methods are often used. Holberg et al. (2008) provided improved distance estimates for DA WDs using multi-band synthetic photometry tied to spectroscopic temperatures and gravities. This method was called Synthetic Spectral Distances (SSD). The unique aspect of SSD is the systematic use of calibrated multi-channel synthetic absolute magnitudes, interpolated within the grid by the  $T_{\text{eff}}$  and  $\log g$ .

$$m_i = \sum_{i=(u,g,r,i,z,V)} M_i(\log g, T_{\text{eff}}) + a_i A_g + 5 \log d - 5 \quad (1)$$

In this paper, the distances of WDs in our sample were estimated using Equation 1. Here,  $m_i$  are the photometric magnitudes of the WDs. Most of our has  $u, g, r, i, z$  magnitudes. Almost all have at least  $g, r$  and  $i$  magnitudes. A few WDs still only have  $V$  magnitude.  $M_i$  is the model absolute magnitudes calculated by interpolations in the atmospheric models provided by Bergeron.  $A_g a_i$  is the reddening and  $d$  is the distance in parsecs. In general for each magnitude a corresponding distance can be calculated. The final distance is estimated by using weighted average. The weights adopted are the errors in the magnitude. Here, we only calculated the distances for WDs having  $u, g, r, i, z$  or  $V$  magnitude data. Distances for two WDs in Table 1 could not be estimated.

## 4. Kinematics

Oppenheimer et al. (2001) suggested that halo WDs could provide a significant contribution to the Galactic dark matters component, which prompted much interest in WD kinematics. In a related study, Silvestri et al. (2002) observed 116 common proper-motion binaries consisting of a WD plus M dwarf component. They determined full space motions of their WDs from the companion M dwarfs. Most of their WDs were found to be members of the disk; only one potential halo WD was identified. Even the much larger samples of WDs such as the Pauli et al. (2003, 2006) SN Ia Progenitor Survey (SPY) have found relatively few genuine halo and thick disk candidates. In their magnitude-limited sample of 398 WDs, they examined both the UVW space motions and the Galactic orbits of their stars. They found only 2% of their sample kinematically belonged to the halo and 7% to the thick disk.

Sion et al. (2009) presented the kinematical properties of the WDs within 20 pc of the Sun. In their nearby sample, they found no convincing evidence of halo members among 129 WDs, nor was there convincing evidence of genuine thick disk subcomponent members within 20 parsecs. The entire 20 pc sample likely belongs to the thin disk.

The proper motions of our sample were derived by the cross-correlating with PPMXL catalog (Roeser et al. 2010). Silvestri et al. (2002); Pauli et al. (2003, 2006), Sion et al. (2009) found relatively little kinematical difference among the samples whether they used radial velocity (RV) to compute full space motions or used the simple zero RV for simple WDs. We have assumed zero RVs in the analysis of our sample.  $U$  is measured positive in the direction of the Galactic anti-center,  $V$  is measured positive in the direction of the Galactic rotation, and  $W$  is measured positive in the direction of the north Galactic pole. The  $U$ ,  $V$  and  $W$  velocities were corrected for the peculiar solar motion  $(U, V, W) = (-9, +12, +7)$  km s<sup>-1</sup> (Wielen 1982). The space motions of 59 WDs with sufficient kinematical information (photometric or trigonometric parallax, proper motion) in our sample were calculated.

The top panel of Fig. 6 shows contours, centered at  $(U, V) = (0, -220)$  km s<sup>-1</sup>, that represent  $1\sigma$  and  $2\sigma$  velocity ellipsoids for stars in the Galactic stellar halo as defined by Chiba & Beers (2000). Only one of our candidate WDs lies outside the  $2\sigma$  velocity contour centered on  $(U, V) = (0, -35)$  km s<sup>-1</sup> defined for disk stars (Chiba & Beers 2000). The bottom of Fig. 6 shows a Toomre diagram for our stars. Venn et al. (2004) suggested stars with  $V_{total} > 180$  km s<sup>-1</sup> are possible halo members. None of our stars meet this criterion. We conclude that our sample consists entirely of disk stars.

Wegg & Phinney (2012) concluded that kinematical dispersion decreases with increasing WD mass among young WDs whose cooling time is smaller than  $3 \times 10^8$  years. Progenitors of high mass WDs have shorter lifetimes, hence they should be closer to the Galactic plane and have small kinematical dispersion in accord with the disk ‘heating’ theory. Since most WDs in our sample are relative young, we investigated the relation between mass and  $W$ , as well as mass and vertical distance of Galactic plane  $|Z|$  (see Fig. 7). In the top panel of Fig. 7, WDs with mass larger than  $0.8 M_{\odot}$  are seen to have smaller  $W$ . Also, the vertical distances from the Galactic plane of WDs with larger mass are relative small. Although there is no strict relation such as seen in Wegg & Phinney (2012), our sample support the general expectation that high mass WDs tend to have lower  $W$  and  $|Z|$ .

## 5. Conclusions

From the LAMOST pilot survey data, 72 DA WDs were detected with  $S/N > 10$ .  $T_{\text{eff}}$ ,  $\log g$ , cooling time, mass and distance of these WDs were determined from their spectra. The  $T_{\text{eff}}$  of most WDs range from 12000 K to 35000 K and the cooling times of all the WDs are younger than 300 Myr. All these WDs were found to be members of Galactic disk. WDs with higher mass tend to have smaller vertical distance from the Galactic disk, which partly supports the conclusions of Wegg et al. (2012).

The DA WD catalogue of the LAMOST pilot survey provides a first glimpse of how useful the survey will be to search for nearby WDs. The upcoming formal LAMOST survey will enlarge the sample of WDs rapidly, perhaps providing the largest sample of WDs available. This large sample will open the door to much more detailed investigation of the physical & kinematic properties of WDs in the solar neighborhood as well as the local structure and evolution of the Galaxy.

Many thanks to D. Koester for providing his WD models. Balmer/Lyman lines in the models were calculated with the modified Stark broadening profiles of Tremblay & Bergeron (2009), kindly made available by the authors. This study is supported by the National Natural Science Foundation of China under grant No. 11233004, 11078019 and 10973021. T.D.O. acknowledges support from NSF grant AST-0807919 to Florida Institute of Technology. Guoshoujing Telescope (the Large Sky Area Multi-Object Fiber Spectroscopic Telescope LAMOST) is a National Major Scientific Project built by the Chinese Academy of Sciences. Funding for the project has been provided by the National Development and Reform Commission. LAMOST is operated and managed by the National Astronomical Observatories, Chinese Academy of Sciences.

## REFERENCES

- Carlin, J. L., Lépine, S., Newberg, H. J., et al. 2012, RAA (Research in Astronomy and Astrophysics), 12, 755
- Chen, L., Hou, J., Yu, J., et al. 2012, RAA(Research in Astronomy and Astrophysics), 12, 805
- Chiba, M., & Beers, T. C., 2000, AJ, 119, 2843
- Cui, X., Zhao, Y., Chu, Y., et al. 2012, RAA(Research in Astronomy and Astrophysics), 12, 1197

- Eisenstein, D. J., Liebert, J., Harris, H. C., et al. 2006, ApJS, 167, 40
- Fontaine, G., Brassard, P., & Bergeron, P. 2001, PASP, 113, 409
- Harris, H. C. et al., 2003, AJ, 126, 1023
- Holberg, J. B., Bergeron, P., & Gianninas, A. 2008, AJ, 135, 1239
- Kleinman, S. J., Harris, H. C., Eisenstein, D. J., et al. 2004, ApJ, 607, 426
- Kleinman, S. J., Kepler, S. O., Koester, D. et al. 2013, ApJS, 204, 5
- Koester, D., 2010, to appear in Mem.S.A.I., based on lectures given at the School of Astrophysics "F. Lucchin", Tarquinia, June 2008 eprint arXiv:0812.0482
- Krziesinski, J., Kleinman, S. J., Nitta, A., Hügelmeyer, S., Dreizler, S., Liebert, J., & Harris, H. 2009, A&A, 508, 339
- Luo, A. L., Zhang, Y. X., & Zhao, Y. H. 2004, in Society of Photo-Optical Instrumentation Engineers (SPIE) Conference Series, vol. 5496, eds. H. Lewis & G. Raffi, 756
- Luo, A. L., Zhang, H. T., Zhao, Y. H, et al. 2012, RAA(Research in Astronomy and Astrophysics), 12, 9
- Markwardt, C. B., 2008, "Non-Linear Least Squares Fitting in IDL with MPFIT," in proc. Astronomical Data Analysis Software and Systems XVIII, Quebec, Canada, ASP Conference Series, Vol. 411, eds. D. Bohlender, P. Dowler & D. Durand (Astronomical Society of the Pacific: San Francisco), p. 251-254 (ISBN: 978-1-58381-702-5; ADS Bibcode: 2009ASPC..411..251M (click for Bibtex and other citation formats) Arxiv preprint: arXiv:0902.2850v1
- Mccook, E. P., & Sion, E. M. 1999, ApJS, 121, 1
- Oppenheimer, B. R., Hambly, N. C., Digby, A. P., Hodgkin, S. T., & Saumon, D. 2001, Science, 292, 698
- Pauli, E.-M., Napiwotzki, R., Heber, U., Altmann, M., & Odenkirchen, M., 2006, A&A, 447, 173
- Pauli, E.-M., Napiwotzki, R., Altmann, M., Heber, U., & Odenkirchen, M. 2003, A&A, 400, 877
- Roeser, S., Demleitner, M., & Schilbach E. 2010, AJ, 139, 2440



- Salaris, M., Garca-Berro, E., Hernanz, M., Isern, J., & Saumon, D. 2000, *ApJ*, 544, 1036
- Schlegel, D. J., Finkbeiner, D. P., & Davis, M. 1998, *ApJ*, 500, 525
- Sion, E. M., Holberg, J. B., Oswalt, T. D., McCook, G. P., & Wasatonic, R. 2009, *AJ*, 138, 1681
- Silvestri, N., Oswalt, T. D., & Hawley, S. 2002, *AJ*, 124, 1118
- Tremblay, P. E., Bergeron, P., & Gianninas, A. 2011, 730, 128
- Venn, K. A., Irwin, M., Shetrone, M. D., Tout, C. A., Hill, V., & Tolstoy, E., 2004, *AJ*, 128, 1177
- Wang, S. G., Su, D. Q., Chu, Y. Q., Cui, X., & Wang, Y. N. 1996, *Appl. Opt.*, 35, 5155
- Wegg, C., & Phinney, E. S. 2012, *MNRAS*, 426, 427
- Wielen, R. 1982, *Landolt-Börnstein Tables, Astrophysics, Vol. 2C, Sec. 8.4* (Berlin: Springer), 202
- Yang, F., Carlin, J. L., Newberg, H. J., et al. 2012, *RAA (Research in Astronomy and Astrophysics)*, 12, 781
- York, D. G., et al. 2000, *AJ*, 120, 1579
- Zhang, Y., Carlin, J., Liu, C., et al. 2012, *RAA (Research in Astronomy and Astrophysics)*, 12, 792

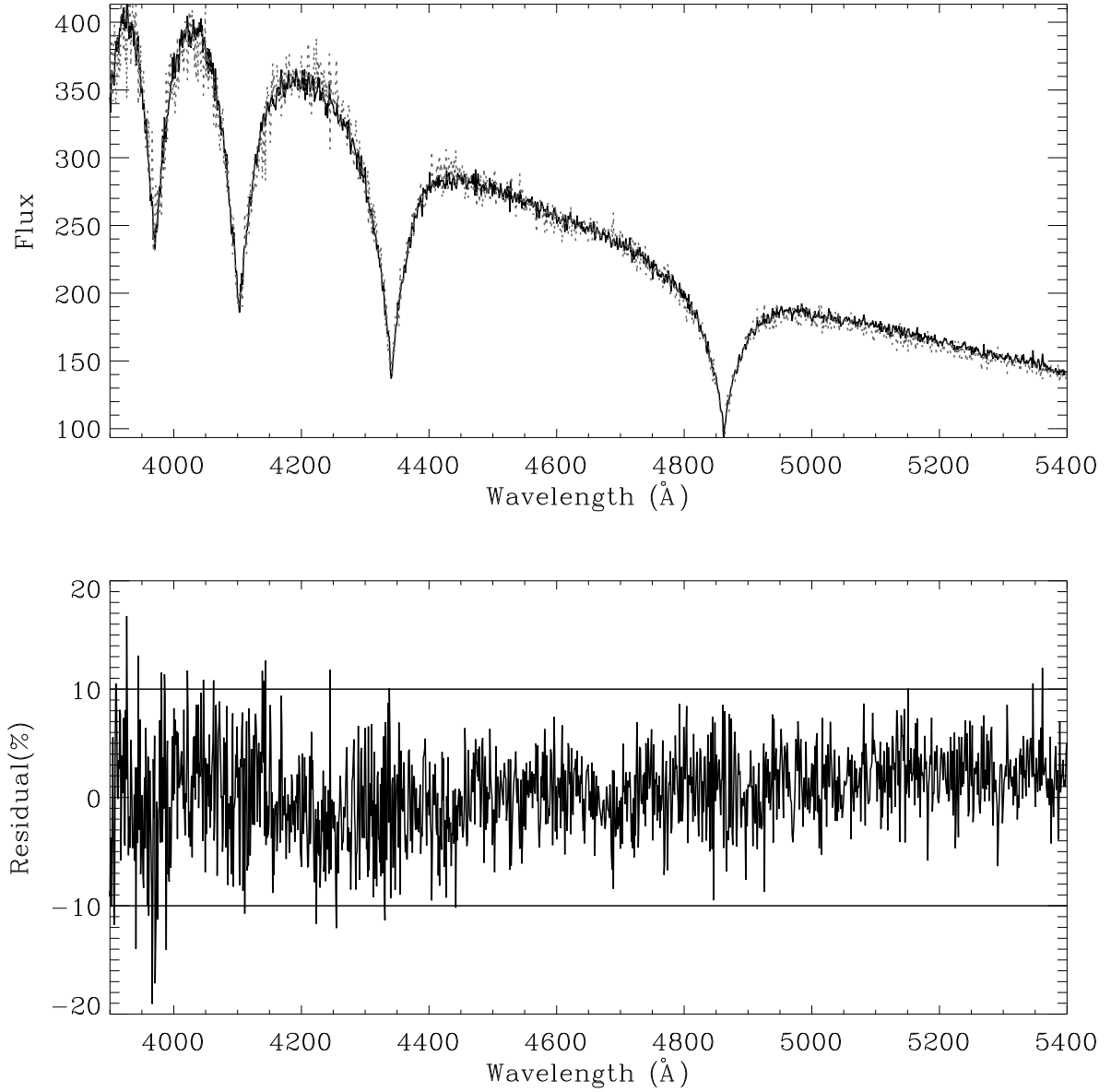


Fig. 1.— A comparison of typical SDSS and LAMOST pilot survey WD spectra for star J100316.35-002336.95. In the top panel, the solid line is the LAMOST spectrum while dotted line is that from SDSS. The bottom panel presents the residue between the two spectra.

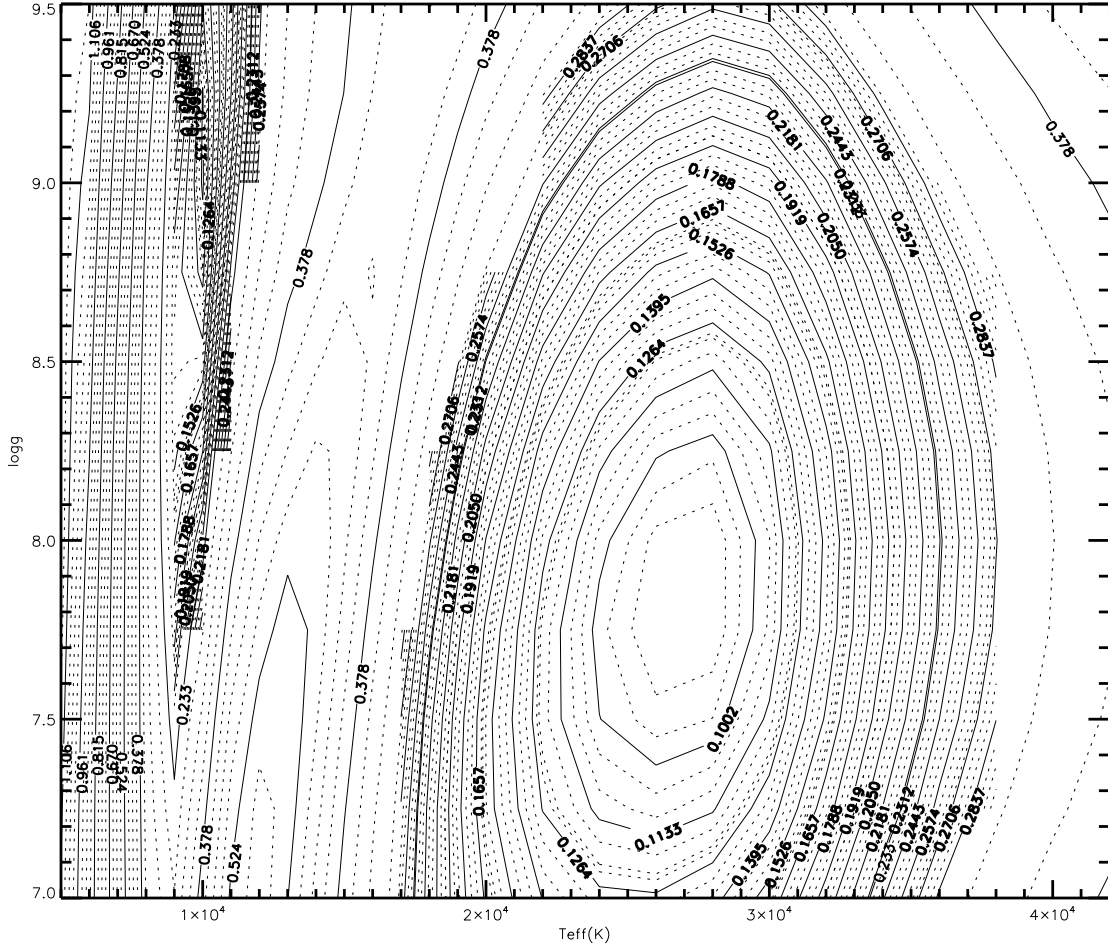


Fig. 2.— The  $\chi^2$  contour plot of  $T_{\text{eff}}$  and  $\log g$  determination.

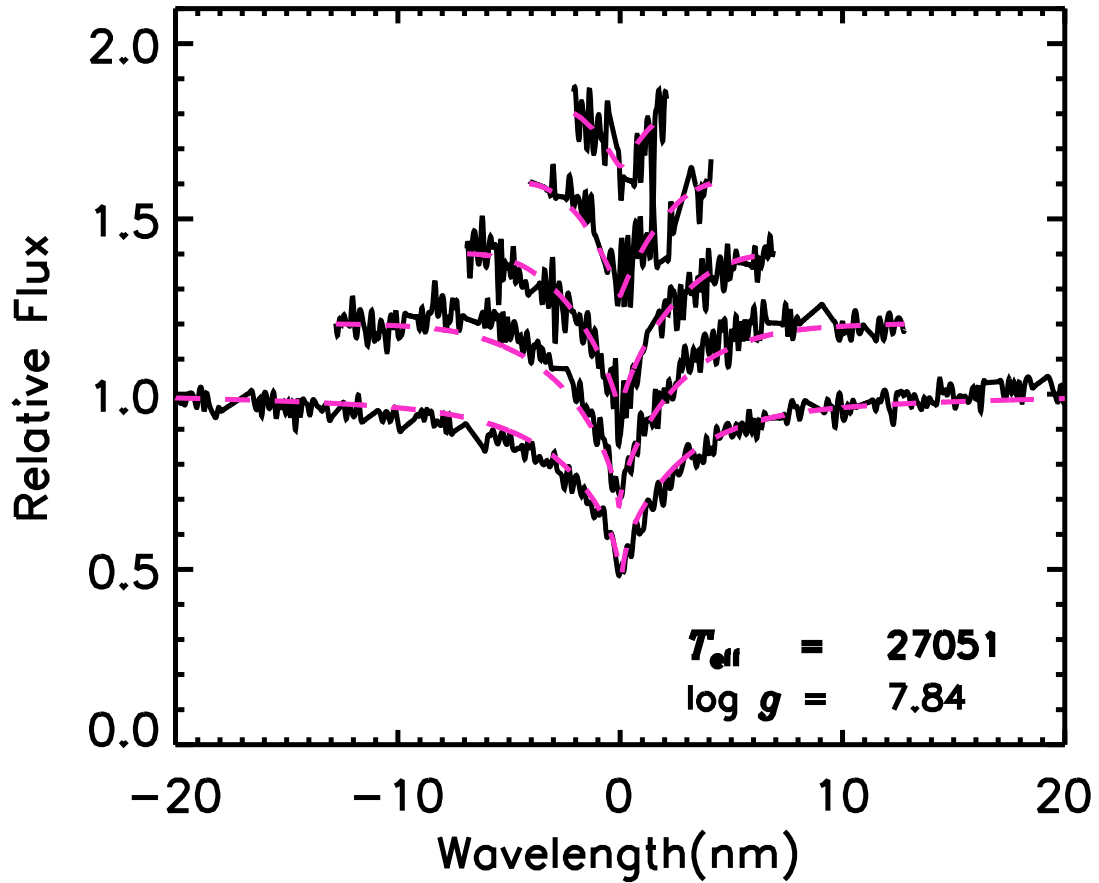


Fig. 3.— Fits of the observed Balmer lines for J150156.26+302300.13. Lines range from H $\beta$  (bottom) to H8 (top). The solid black line is the observed spectra while the dashed line is the model spectra.

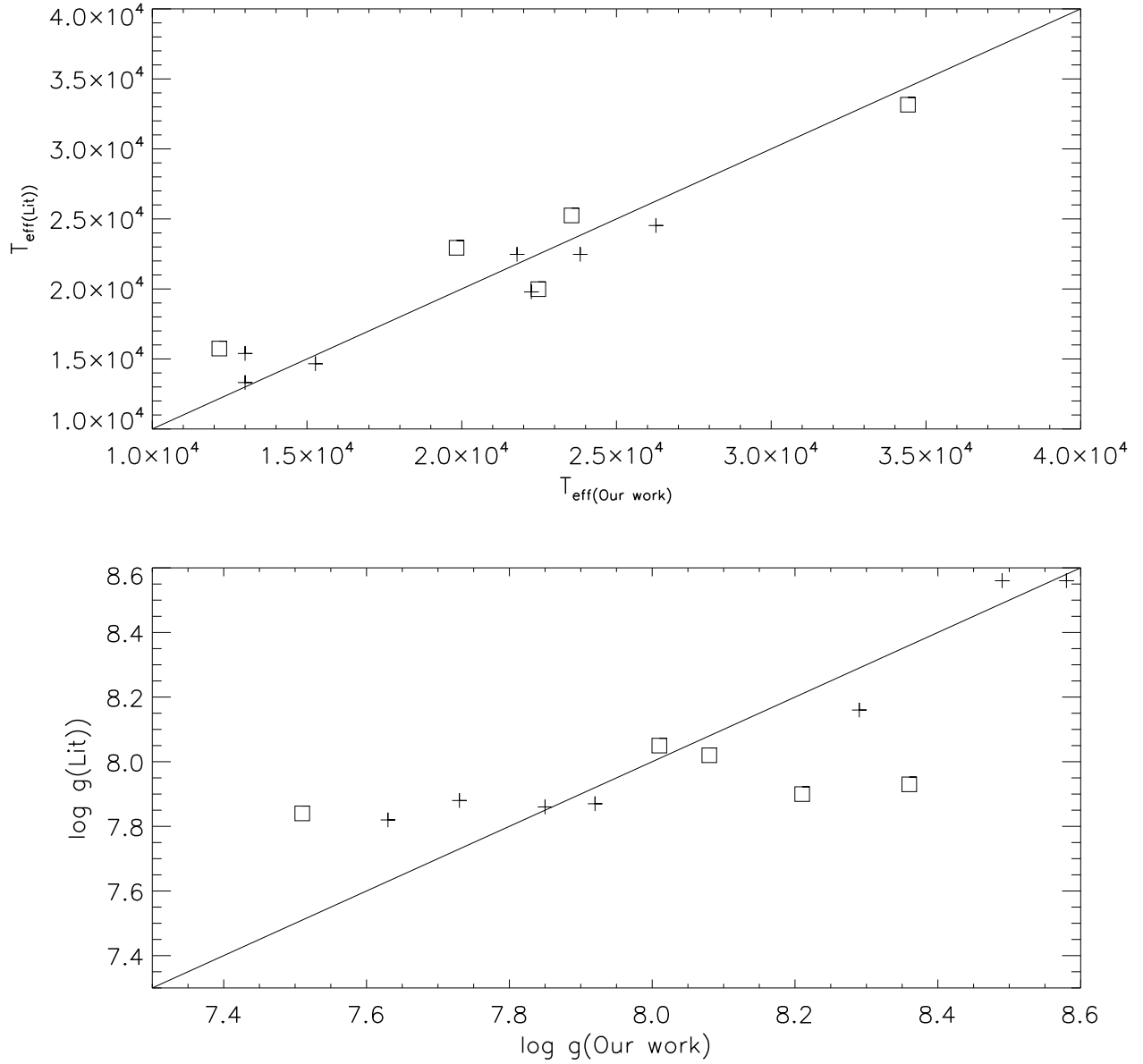


Fig. 4.— Comparison of estimated  $T_{\text{eff}}$  and  $\log g$  values determined in this study to those from the literature. Pluses (+) represent WDs with high S/N ( $>20$ ), while squares represent WDs with low S/N ( $<20$ ) spectra. The solid line is the unit slope relation.

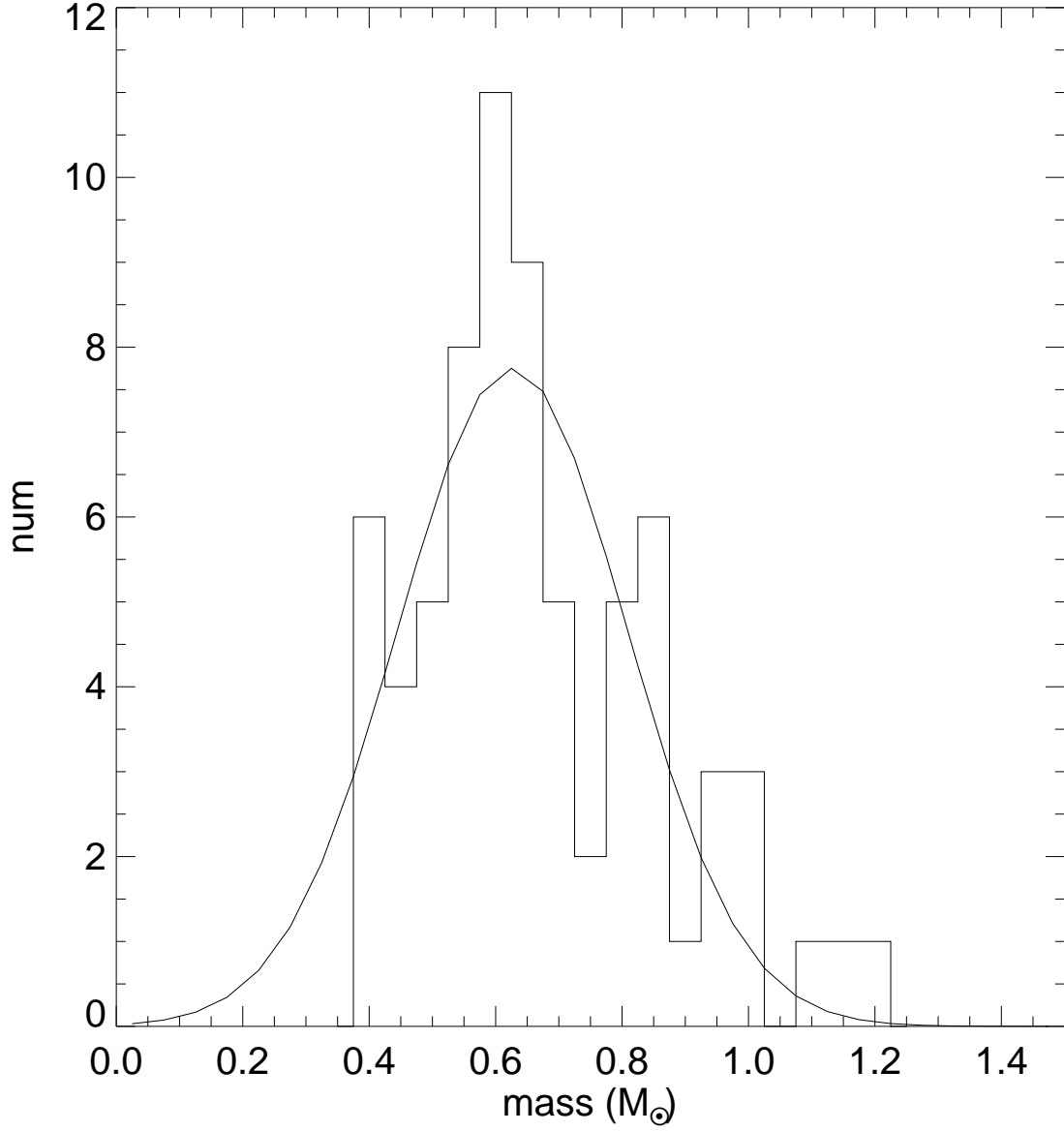


Fig. 5.— Mass distribution of our sample of candidate WDs. The curve is a Gaussian fit with a peak at about  $0.61 M_{\odot}$

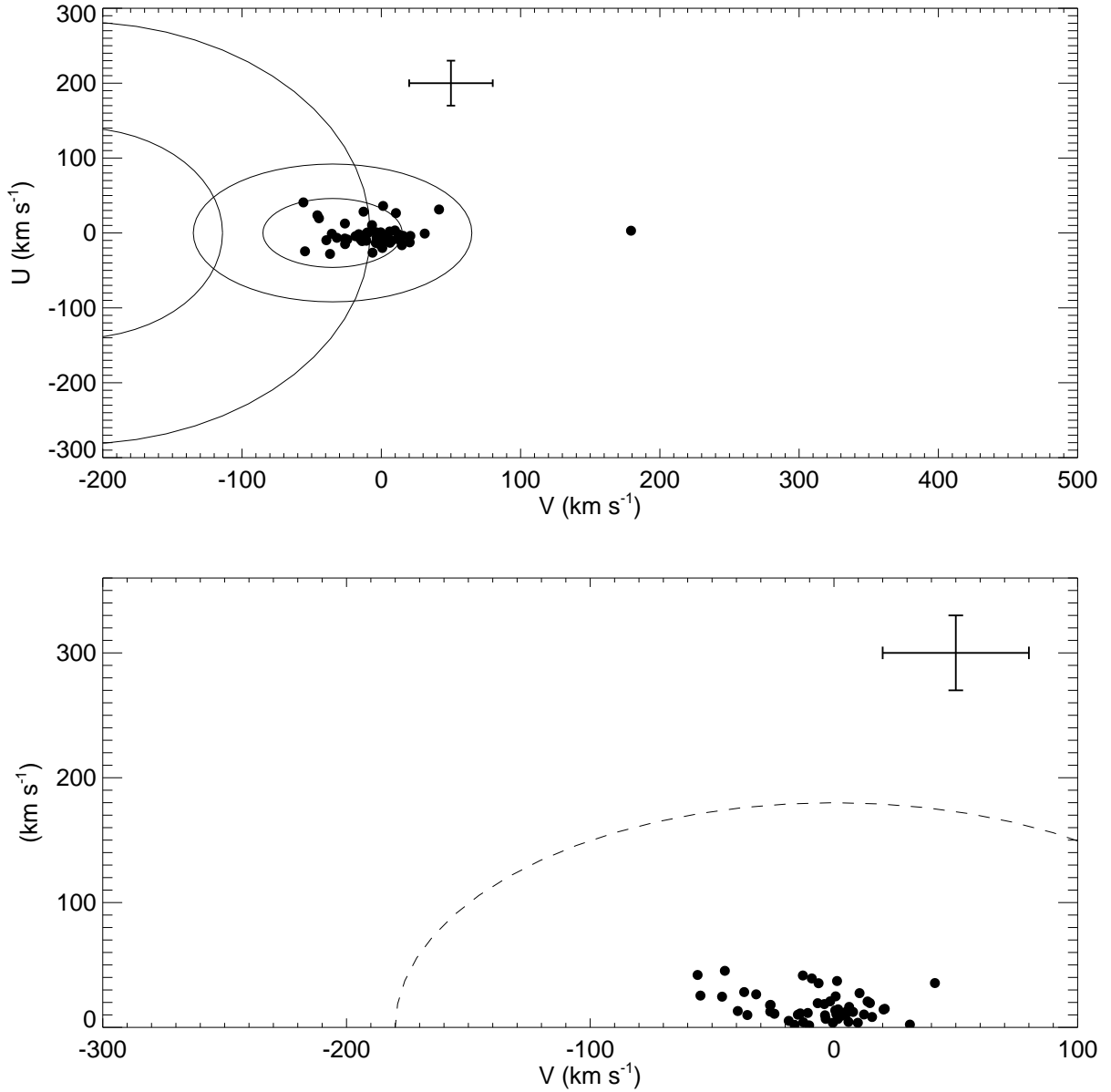


Fig. 6.— Top: UV-velocity distribution of our WD candidates. Ellipsoids indicate  $1\sigma$  (inner) and  $2\sigma$  (outer) contours for Galactic thick disk and halo populations, respectively. Bottom: Toomre diagram of our WDs. Dashed line is  $V_{\text{total}} = 180 \text{ km s}^{-1}$ .

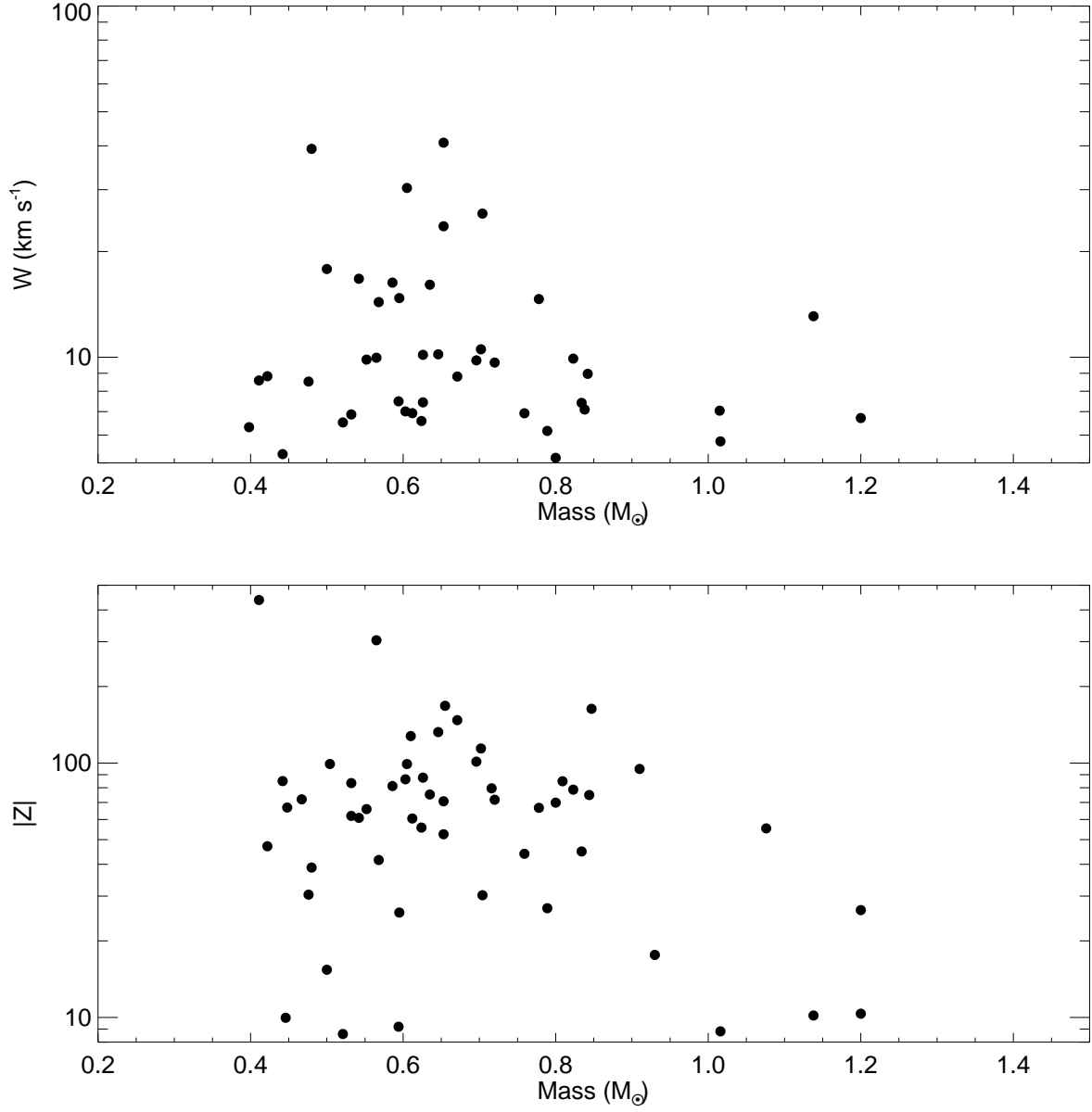


Fig. 7.— Top:  $W$  vs. Mass. Bottom:  $|Z|$  vs. Mass. Lower mass WDs clearly tend to have larger dispersion in both  $W$  velocity and vertical distance of the Galactic plane  $|Z|$ .



Table 1. catalog of DA white dwarfs.

No	LAMOST Obj	RA (deg)	DEC (deg)	T <sub>eff</sub> (K)	log g	mass (M <sub>⊙</sub> )	age (Myr)	u	g	r	i	z	V	source <sup>a</sup>	E(B-V)	dis (pc)
0	J220522.86+021837.56	331.345250	2.310432	15377 ± 493	8.02 ± 0.10	0.63 ± 0.06	190 ± 43	17.35	17.00	17.25	17.45	17.71		1	0.05	135
1	J025737.25+264047.89	44.405201	26.679970	19008 ± 669	7.87 ± 0.12	0.55 ± 0.06	66 ± 21		16.91	17.00	17.16			2	0.16	139
2	J030214.72+285707.41	45.561340	28.952057	21894 ± 1406	8.01 ± 0.23	0.64 ± 0.13	46 ± 37		17.21	17.60	17.80			2	0.18	173
3	J040449.34+280023.65	61.205600	28.006570	29302 ± 2525	8.25 ± 0.55	0.79 ± 0.33	20 ± 32		15.96	15.84	16.00			2	0.21	87
4	J004036.79+413138.79	10.153296	41.527443	13000 ± 651	7.75 ± 0.08	0.48 ± 0.04	216 ± 47		15.90	16.21	16.40			2	0.07	83
5	J003956.55+422929.55	9.985629	42.491542	18053 ± 816	7.32 ± 0.15	0.34 ± 0.05	50 ± 10		16.43	16.58	16.72			2	0.06	181
6	J004128.67+402324.09	10.369458	40.390026	25996 ± 733	7.92 ± 0.10	0.59 ± 0.05	15. ± 3.						17.14	3	0.08	68
7	J005340.53+360116.89	13.418857	36.021358	29772 ± 158	7.96 ± 0.04	0.63 ± 0.02	9 ± 0		14.10	14.58	14.91			2	0.05	72
8	J100551.51-023417.87	151.464628	-2.571630	22072 ± 477	8.22 ± 0.07	0.76 ± 0.04	78 ± 16	15.15	15.10	15.46	15.76	16.08		1	0.05	68
9	J100316.35-002336.95	150.818141	-0.393597	22249 ± 330	7.92 ± 0.05	0.59 ± 0.03	33 ± 4	15.97	15.93	16.25	16.56	16.85		1	0.05	123
10	J100941.45-004404.55	152.422705	-0.734597	16489 ± 601	7.98 ± 0.13	0.60 ± 0.08	140 ± 45	17.36	16.98	17.24	17.44	17.74		1	0.04	148
11	J054613.53+255031.70	86.556364	25.842139	22935 ± 498	7.99 ± 0.07	0.63 ± 0.04	34 ± 10		17.33	17.62	17.78			2	1.72	27
12	J090734.26+273903.32	136.892757	27.650923	18619 ± 386	8.56 ± 0.07	0.97 ± 0.04	272 ± 39	16.31	16.08	16.37	16.64	16.89		1	0.03	72
13	J004628.31+343319.90	11.617971	34.555527	14644 ± 808	7.60 ± 0.18	0.41 ± 0.08	120 ± 47	16.83	16.33	16.40	16.53	16.75		1	0.08	112
14	J005340.53+360116.89	13.418857	36.021358	26534 ± 394	7.88 ± 0.06	0.58 ± 0.03	13 ± 1		14.10	14.58	14.91			2	0.05	67
15	J052038.36+304822.65	80.159836	30.806293	15924 ± 348	8.00 ± 0.07	0.61 ± 0.04	164 ± 28		15.38	15.68	15.88			2	0.85	24
16	J031236.50+515511.74	48.152099	51.919927	23558 ± 1966	7.93 ± 0.29	0.59 ± 0.14	25 ± 13						15.44	3	0.84	103
17	J055046.51+261220.27	87.693772	26.205631	28000 ± 1916	8.34 ± 0.39	0.84 ± 0.24	37 ± 57		15.13	15.64	15.91			2	1.50	13
18	J013938.94+291859.80	24.912266	29.316611	20934 ± 515	8.13 ± 0.08	0.70 ± 0.05	77 ± 22		17.53	17.94	18.19			2	0.05	213
19	J105811.27+475752.75	164.546942	47.964653	29532 ± 490	7.84 ± 0.11	0.56 ± 0.05	9 ± 0	17.09	17.29	17.75	18.10	18.35		1	0.01	353
20	J104311.45+490224.35	160.797708	49.040097					15.47	15.84	16.40	16.76	17.18		1	0.01	
21	J053931.86+285456.66	84.882770	28.915740	23865 ± 1774	8.63 ± 0.26	1.01 ± 0.15	147 ± 97		17.39	16.64	16.17			2	1.43	15
22	J094104.43+282224.58	145.268457	28.373495	16713 ± 438	7.86 ± 0.09	0.54 ± 0.05	109 ± 24	15.70	15.42	15.70	15.94	16.25		1	0.02	82
23	J081845.28+121952.45	124.688667	12.331236	22271 ± 531	8.34 ± 0.08	0.83 ± 0.05	100 ± 22	16.32	16.18	16.57	16.88	17.19		1	0.03	107
24	J014147.59+302135.45	25.448307	30.359846	17520 ± 367	8.17 ± 0.07	0.72 ± 0.04	162 ± 27		16.96	17.39	17.54			2	0.05	138
25	J014933.76+285610.60	27.390679	28.936279	32200 ± 631	8.33 ± 0.12	0.84 ± 0.07	17 ± 10		16.88	17.47				2	0.06	140
26	J074742.05+280945.57	116.925192	28.162658	15085 ± 596	7.66 ± 0.13	0.44 ± 0.06	117 ± 31	17.83	17.43	17.69	17.88	18.13		1	0.04	209
27	J075251.35+271513.85	118.213962	27.253847	25134 ± 711	7.94 ± 0.10	0.60 ± 0.06	19 ± 9	16.72	16.73	17.15	17.46	17.79		1	0.03	206
28	J075106.48+301726.96	117.776979	30.290822	34418 ± 580	8.21 ± 0.10	0.78 ± 0.06	9 ± 1	15.65	15.92	16.39	16.72	17.05		1	0.05	156
29	J113614.04+290130.26	174.058504	29.025072	24106 ± 255	7.80 ± 0.03	0.53 ± 0.02	20 ± 1	14.64	14.68	15.13	15.44	15.75		1	0.02	87
30	J113705.17+294757.54	174.271529	29.799317	21786 ± 160	8.58 ± 0.03	0.98 ± 0.02	174 ± 11	12.29	12.31	12.69	12.99	13.31		1	0.02	15
31	J113423.35+314606.58	173.597300	31.768494	14683 ± 832	8.02 ± 0.14	0.62 ± 0.08	219 ± 73	15.53	15.17	15.44	15.68	15.95		1	0.03	58
32	J093903.33+114418.62	144.763879	11.738506	16673 ± 815	8.75 ± 0.09	1.08 ± 0.05	513 ± 116	17.37	17.01	17.21	17.41	17.67		1	0.03	82
33	J070755.01+265102.94	106.979210	26.850817	17854 ± 893	8.87 ± 0.12	1.14 ± 0.06	554 ± 202		15.53	15.86	16.01			2	0.07	39

Table 1—Continued

No	LAMOST Obj	RA (deg)	DEC (deg)	T <sub>eff</sub> (K)	log g	mass (M <sub>⊙</sub> )	age (Myr)	u	g	r	i	z	V	source <sup>a</sup>	E(B-V)	dis (pc)
34	J104946.47+003635.81	162.443625	0.609947	19832 ± 550	8.08 ± 0.10	0.67 ± 0.06	87 ± 23	17.25	17.27	17.67	17.97	18.30		1	0.05	191
35	J104623.28+024236.57	161.596987	2.710158	13000 ± 728	7.73 ± 0.08	0.47 ± 0.04	211 ± 52	16.43	16.03	16.26	16.48	16.72		1	0.04	92
36	J104928.89+275423.77	162.370375	27.906603	14212 ± 681	7.68 ± 0.15	0.45 ± 0.07	148 ± 44	15.74	15.32	15.51	15.75	15.98		1	0.02	75
37	J115506.22+264924.59	178.775929	26.823497	17291 ± 679	8.47 ± 0.13	0.91 ± 0.08	285 ± 88	17.03	16.69	16.97	17.23	17.50		1	0.02	97
38	J094627.81+313211.08	146.615867	31.536411	15000 ± 2362	8.34 ± 0.20	0.82 ± 0.13	342 ± 218	17.30	16.91	17.12	17.34	17.55		1	0.02	103
39	J070057.53+284310.06	105.239692	28.719461	16000 ± 735	8.15 ± 0.13	0.70 ± 0.08	207 ± 66	17.37	16.98	17.23	17.45	17.73		1	0.08	120
40	J040613.25+465133.66	61.555205	46.859349	33026 ± 436	7.50 ± 0.10	0.45 ± 0.03	6 ± 1						14.77	3	0.82	145
41	J103535.22+395502.27	158.896764	39.917298	16652 ± 550	8.05 ± 0.11	0.65 ± 0.07	155 ± 39	17.43	17.12	17.33	17.55	17.84		1	0.01	154
42	J105443.36+270658.42	163.680650	27.116228	24915 ± 131	8.38 ± 0.02	0.86 ± 0.02	74 ± 4	13.86	13.98	14.34	14.64	14.97		1	0.02	41
43	J064452.84+260947.75	101.220170	26.163263	16835 ± 598	7.78 ± 0.13	0.50 ± 0.06	90 ± 20		15.48	15.98	16.22			2	0.10	86
44	J065601.55+115745.85	104.006460	11.962736	31347 ± 603	7.42 ± 0.15	0.41 ± 0.05	8 ± 1		14.31	13.48	13.13	11.94		1	0.22	63
45	J013914.45+290057.61	24.810197	29.016003	16808 ± 478	8.06 ± 0.10	0.65 ± 0.06	153 ± 34		16.20	16.53	16.68			2	0.06	97
46	J094126.79+294503.39	145.361630	29.750942	21798 ± 267	8.15 ± 0.04	0.72 ± 0.03	68 ± 10	15.88	15.91	16.25	16.55	16.87		1	0.02	106
47	J100549.01+424804.68	151.454200	42.801300	23923 ± 812	8.11 ± 0.12	0.70 ± 0.07	38 ± 13	16.04	16.00	16.39	16.70	16.98		1	0.01	127
48	J093047.11+160012.98	142.696300	16.003606	32492 ± 634	8.00 ± 0.13	0.66 ± 0.07	7 ± 1	16.35	16.64	17.12	17.50	17.84		1	0.04	249
49	J093451.69+171814.00	143.715358	17.303889	14645 ± 566	7.80 ± 0.12	0.50 ± 0.06	156 ± 45	17.10	16.79	17.09	17.36	17.66		1	0.03	143
50	J092518.36+180534.20	141.326500	18.092833	26274 ± 324	8.29 ± 0.06	0.81 ± 0.04	43 ± 11	16.07	16.17	16.61	16.94	17.23		1	0.05	127
51	J052147.24+283532.50	80.446823	28.592361	18917 ± 466	7.81 ± 0.09	0.52 ± 0.05	59 ± 16		17.50	17.73	17.86			2	0.62	108
52	J071223.81+260933.41	108.099190	26.159281	14278 ± 632	7.75 ± 0.14	0.48 ± 0.06	159 ± 40		16.85	17.24	17.41			2	0.08	141
53	J102521.36+455553.91	156.338987	45.931643	23547 ± 908	7.51 ± 0.13	0.41 ± 0.05	19 ± 3	18.12	18.27	18.60	18.89	19.26		1	0.02	530
54	J101806.60+455830.36	154.527482	45.975101	22475 ± 1541	8.36 ± 0.22	0.85 ± 0.14	101 ± 59	17.61	17.55	17.90	18.19	18.47		1	0.01	201
55	J033149.69+305944.92	52.957023	30.995811	19435 ± 332	8.64 ± 0.06	1.02 ± 0.03	277 ± 37		16.89	17.41	17.67			2	1.18	25
56	J033253.91+284006.91	53.224625	28.668586	19000 ± 1400	9.84 ± 0.09	1.20 ± 0.15	155 ± 0		17.06	17.41	17.58			2	0.25	27
57	J090918.99+292929.61	137.329125	29.491558	22588 ± 346	8.04 ± 0.05	0.65 ± 0.03	43 ± 8	15.74	15.68	16.04	16.34	16.59		1	0.02	107
58	J102155.50+405014.85	155.481261	40.837458	23364 ± 999	7.96 ± 0.15	0.61 ± 0.09	28 ± 18	16.19	16.25	16.61	16.91	17.23		1	0.01	153
59	J121336.54+314808.77	183.402250	31.802436	13308 ± 405	8.26 ± 0.08	0.77 ± 0.05	418 ± 67	16.21	15.79	16.00	16.21	16.49		1	0.01	60
60	J134922.51-003503.15	207.343783	-0.584208	16401 ± 1151	8.52 ± 0.19	0.94 ± 0.12	363 ± 153	17.24	16.91	17.25	17.46	17.73		1	0.03	99
61	J144433.83-005958.83	221.140967	-0.999675	12165 ± 856	8.01 ± 0.21	0.61 ± 0.13	367 ± 154	16.58	16.20	16.38	16.58	16.85		1	0.04	77
62	J112518.85+541936.65	171.328550	54.326847	15272 ± 209	7.85 ± 0.04	0.53 ± 0.02	147 ± 14	15.62	15.28	15.57	15.83	16.08		1	0.01	73
63	J113203.47+065509.52	173.014441	6.919311	12455 ± 1141	7.93 ± 0.45	0.57 ± 0.25	310 ± 201	15.21	14.89	15.13	15.35	15.64		1	0.04	46
64	J084107.69+163221.71	130.282053	16.539363	16626 ± 580	8.30 ± 0.11	0.80 ± 0.07	237 ± 64	17.52	17.22	17.45	17.67	17.97		1	0.02	134
65	J150156.26+302300.13	225.484400	30.383369	27051 ± 339	7.84 ± 0.05	0.56 ± 0.03	12 ± 1	14.13	14.24	14.71	14.96	15.32		1	0.02	77
66	J063406.26+025401.30	98.526074	2.900361	31607 ± 1274	7.82 ± 0.31	0.56 ± 0.14	7 ± 1							4	1.60	
67	J064438.16+030704.39	101.159020	3.117885	12067 ± 2288	8.37 ± 0.65	0.84 ± 0.42	650 ± 791		14.10	13.66	13.51			2	1.02	5

Table 1—Continued

No	LAMOST Obj	RA (deg)	DEC (deg)	$T_{\text{eff}}$ (K)	$\log g$	mass ( $M_{\odot}$ )	age (Myr)	u	g	r	i	z	V source <sup>a</sup>	E(B-V) dis (pc)
68	J063517.47+054917.94	98.822796	5.821650	22885. $\pm$ 3739	7.48 $\pm$ 0.54	0.40 $\pm$ 0.14	21 $\pm$ 13		14.19	13.96	13.84		2	0.41 38
69	J152130.83-003055.70	230.378443	-0.515472	13000 $\pm$ 1056	7.63 $\pm$ 0.10	0.42 $\pm$ 0.05	186. $\pm$ 71.	15.52	15.24	15.53	15.78	16.09	1	0.07 67
70	J113705.14+294757.77	174.271408	29.799381	23829 $\pm$ 127	8.49 $\pm$ 0.02	0.93 $\pm$ 0.02	111 $\pm$ 6	13.54	12.45	12.88	13.16	13.69	1	0.02 18
71	J191927.67+395839.30	289.865292	39.977583	20376 $\pm$ 345	7.93 $\pm$ 0.06	0.59 $\pm$ 0.03	54 $\pm$ 8						4	0.14

<sup>a</sup>1: SDSS 2: Xuyi Schmidt Telescope Photometric Survey of the Galactic Anti-center 3: UCAC 4: Kepler